Research Square

Preprints are preliminary reports that have not undergone peer review.
They should not be considered conclusive, used to inform clinical practice,
or referenced by the media as validated information.

Development of an infectious clone of papaya virus Q and evaluation of its potential as a virus-induced gene silencing (VIGS) vector

Nelson Cubi-Insuaste
Escuela Superior Politecnica del Litoral
Milenka Vera
University of Minnesota
Sara Zurita
University of Minnesota
Raul Cifuentes
University of Arkansas
Robert A. Alvarez-Quinto
University of Minnesota
Diego F. Quito-Avila
dquito@espol.edu.ec

Escuela Superior Politecnica del Litoral

Research Article

Keywords: Umbra-like virus, Group 1/Class 2, PDS-papaya

Posted Date: September 4th, 2026

DOI: https://doi.org/10.21203/rs.3.rs-10820954/v1

License: This work is licensed under a Creative Commons Attribution 4.0 International License.
Read Full License

Additional Declarations: No competing interests reported.

Abstract

Papaya virus Q (PpVQ) is the type member of Group 2/Class 1 umbra-like viruses associated with papaya but has not been fully characterized in single infections. In this study, RACE analysis identified two alternative 3'-terminal sequences of PpVQ, both of which supported systemic infection in *Nicotiana benthamiana* and papaya. One variant, PpVQ_V2, shared an 8-nt terminal sequence with the closely related babaco virus Q. Although PpVQ_V2 tolerated the insertion of three phytoene desaturase (PDS) sequences and established systemic infection, the inserts were progressively lost during infection. Deletion variants emerged by 5 weeks post-agroinfiltration, and sequencing revealed a reproducible modified junction in which part of the PDS insert and adjacent viral sequence were deleted. No visible PDS-silencing phenotype was observed in either host. These results demonstrate that PpVQ can transiently accommodate heterologous sequences but exhibits limited stability of the tested inserts, providing new insights into PpVQ genome plasticity and constraints relevant to its potential development as a VIGS vector.

Introduction

Papaya virus Q (PpVQ) is the prototype member of Group 2/Class 1 umbra-like viruses (ULVs) and was first identified in papaya (*Carica papaya*) in co-infections with papaya ringspot virus (PRSV) [1]. Genome sequencing revealed that PpVQ had a positive-sense RNA genome of approximately 4.3 kb containing only two recognizable open reading frames (ORFs): ORF1, encoding a protein of unknown function, and ORF2, encoding the RNA-dependent RNA polymerase (RdRp), hypothetically expressed through a -1 frameshifting mechanism [1–3]. An intriguing genomic feature of PpVQ is the presence of an unusually long (~ 1.8 kb) 3' untranslated region (UTR), which is likely an evolutionary vestige from tombusvirid ancestors [4].

Although the virus is frequently detected in mixed infections with PRSV and is associated with field spread by the whitefly *Bemisia tabaci* [2], no consistent symptoms have been unequivocally attributed to PpVQ infection. Since its discovery, closely related Group 2/Class 1 ULVs have been identified in papaya and other members of the Caricaceae, including babaco (*Vasconcellea × heilbornii*) [3, 5], with reports of their presence throughout Latin America and Australia, suggesting that this lineage is distributed worldwide [6]. Nevertheless, the precise roles of PpVQ and related viruses in symptom expression, host adaptation, virus movement, and virus evolution remain poorly understood.

To date, reverse genetic studies of umbra-like viruses have been largely restricted to Group 2/Class 2 members, particularly *Citrus yellow vein associated virus* (CY1) [7]. An infectious clone of CY1 demonstrated that this virus is independently infectious and systemically infects several experimental hosts in the absence of a helper virus. More importantly, the clone has enabled detailed studies of viral replication, RNA structural elements, and host-virus interactions, and was successfully engineered as a virus-induced gene silencing (VIGS) vector [8, 9] illustrating the power of infectious clone technology for elucidating the biology of umbra-like viruses while providing versatile platforms for functional genomics.

Despite the increasing recognition of Class 1 ULVs as widespread and biologically relevant viruses of papaya, no reverse genetic system has been developed for this lineage. The compact genome of PpVQ, its apparent ability to establish systemic yet largely asymptomatic infections, and its natural adaptation to papaya make it an attractive candidate for the development of a viral vector. In addition to advancing our understanding of Group 2/Class 1 ULV biology, a PpVQ-based infectious clone could provide a much-needed tool for functional genomic studies in papaya, a crop for which efficient reverse genetic approaches remain limited.

Here, we report the construction and biological characterization of the first infectious clone of a Group 2/Class 1 umbra-like virus. We demonstrate the infectivity of the PpVQ clone, characterize its biological properties, and evaluate its potential as a virus-induced gene silencing vector for functional genomics in papaya.

Materials and Methods

Virus isolate and genome confirmation

PpVQ isolate Cent2 (GenBank accession no. MT113180), originally collected and sequenced in 2017, was used throughout this study. To confirm the viral terminal sequences, the original sample, archived at − 80°C, was subjected to rapid amplification of cDNA ends (RACE) using two virus-specific primers for each genome end following the manufacturer's instructions (Roche). Amplified products were cloned into the pGEM-T vector (Promega, USA) and Sanger sequenced.

Plant material and virus detection

All inoculation assays were performed using virus-free *Carica papaya* cv. Sunrise and *Nicotiana benthamiana* plants grown under greenhouse conditions (25°C, 12-h photoperiod) inside insect-proof cages.

Total RNA was extracted from approximately 80 mg of young, fully expanded leaf tissue using a lithium chloride-based extraction buffer followed by clarification with potassium acetate, isopropanol precipitation, and RNA capture using glass milk as previously described [10, 11].

For conventional RT-PCR, reverse transcription was performed in a 15-µL reaction containing 80 ng of total RNA, 1 µM random primers, and 40 U of Scriptase II reverse transcriptase (Nippon Genetics Co., Japan), according to the manufacturer's instructions. PCR amplification was carried out using FastGene® Taq 2× Ready Mix (Nippon Genetics Co., Japan) in 10-µL reactions containing 1 µL of cDNA and 0.8 µM of each of the PpVQ-specific primers described previously [1].

To compare viral RNA accumulation among infectious clone constructs, a TaqMan™ RT-qPCR assay was developed using the TaqMan™ Fast Virus 1-Step Master Mix (Thermo Fisher Scientific, USA) and

performed on an Applied Biosystems QuantStudio™ 5 Real-Time PCR System. Assay efficiency was evaluated using 10-fold serial dilutions of DNase-treated RNA extracted from a PpVQ-infected papaya plant. Transcript levels were normalized against the papaya NADH dehydrogenase subunit B (ndhB) gene using the primers and probe described previously [12]. Following validation of assay efficiency, relative viral RNA accumulation was calculated using the 2^−ΔΔCt method [13]. Technical replicates (n = 3) were averaged for each biological replicate (n = 5), and statistical comparisons between PpVQ_V1 and PpVQ_V2 were performed on ΔCt values using Welch's t-test.

Construction of the infectious clone

An infectious cDNA clone was constructed using the complete genomic sequence of PpVQ (GenBank accession no. MT113180) together with the terminal sequences determined in this study. The viral genome was synthesized as three fragments (Twist Bioscience, San Francisco, CA, USA) and assembled into the binary vector pLX-AS using the NEBridge® Golden Gate Assembly Kit (New England Biolabs, USA) following the method of Pasin et al. (2022) [14].

To generate authentic viral 3' termini during in planta transcription, a ribozyme sequence derived from tobacco ringspot virus satellite RNA (GenBank accession no. M14879), containing the last nine nucleotides of the PpVQ genome in reverse-complement orientation, was placed immediately downstream of the viral genome.

The resulting pLX-AS_PpVQ construct was transformed into One Shot™ TOP10 electrocompetent *Escherichia coli* cells. Positive transformants were identified by colony PCR using primers 698F/698R [1]. Single colonies were grown overnight, and plasmid DNA was purified using the ZymoPURE Plasmid Miniprep Kit (Zymo Research, USA).

Agroinfiltration

Purified plasmids were introduced into electrocompetent *Agrobacterium tumefaciens* strain GV2260 by electroporation using a Bio-Rad MicroPulser®. Transformants were selected on YEP agar (1% peptone, 0.5% yeast extract, 0.5% NaCl, 1.5% agar) supplemented with carbenicillin (100 µg mL^{-1}) and kanamycin (50 µg mL^{-1}). PCR-positive colonies were grown overnight in antibiotic-supplemented YEP medium to an OD600 of approximately 2. To confirm that the binary vector remained intact following transfer to *A. tumefaciens*, plasmid DNA recovered from two independent transformants was subjected to Oxford Nanopore PromethION sequencing (Macrogen Inc. South Korea). After sequence confirmation, the corresponding *Agrobacterium* cultures were regrown to an OD600 of ~ 2.

Cells were pelleted (2,600 × g, 10 min), resuspended in infiltration buffer (Murashige and Skoog medium supplemented with 30 mg L^{-1} ascorbic acid, 10 mM 3-(N-morpholino) propanesulfonic acid (MOPS), pH 5.5, and 200 µM acetosyringone), and incubated for 3 h at room temperature in the dark prior to inoculation.

Approximately 500 µL of bacterial suspension was infiltrated into the abaxial surface of two fully expanded leaves using a needleless syringe. In papaya, the suspension was additionally introduced by stem puncture with a sterile toothpick and applied to the margins of two freshly cut leaves as described by Vera et al. (2025) [15].

Following infiltration, plants were maintained under greenhouse conditions (25°C, 12-h photoperiod) and tested for systemic infection by RT-PCR using RNA extracted from non-inoculated leaves. Plants were sampled at different weeks post-agroinfiltration (wpi), depending on the experiment. Each experiment consisted of 10 plants including two negative controls infiltrated either with *A. tumefaciens* carrying the empty pLX-AS vector or the infiltration buffer alone. Each experiment was independently repeated three times, and infection rates are reported based on the combined results of the three independent experiments.

Identification of a VIGS insertion site

A systematic analysis of the PpVQ genome was performed to identify suitable sites for insertion of VIGS sequences. Multiple sequence alignments of complete or near-complete genomes of PpVQ and closely related Group 2/Class 1 umbra-like viruses, including papaya meleira virus 2 (PMeV-2) and PapMeV-Mx, were used to identify conserved regions, which were excluded as potential insertion sites. Reverse-complement repeats (> 9 nt long), identified using the “Find Repeats” tool in Geneious Prime 2025, were also excluded because of their potential to mediate long-distance RNA-RNA interactions. This analysis was complemented by RNA secondary structure predictions across the PpVQ genome using the RNAfold WebServer and visualized with RNA Canvas [16]. Candidate regions were evaluated based on their predicted secondary structures, base-pairing probabilities, and positional entropy (PE) to assess the structural context and conformational variability of individual nucleotides as documented for related viruses [17].

Design of VIGS vectors

A single insert targeting a conserved region of the phytoene desaturase (*PDS*) gene of papaya and *Nicotiana benthamiana* was designed based on a pairwise alignment of *PDS* sequences from both species. The target region was amplified using primers designed from publicly available sequences (papaya, DQ779922; *N. benthamiana*, DQ469932 and LC543533; Online Resource 1). The predicted effect of this insert on the local RNA secondary structure at the selected insertion site was evaluated to minimize disruption of the viral RNA structure. For papaya, two additional inserts were subsequently designed and evaluated using the same structural criterion, with the aim of identifying alternative inserts with potentially greater compatibility with the local viral RNA structure. Each insert was introduced into the previously identified insertion site (see above) within the third synthetic viral genomic fragment (Twist Bioscience, San Francisco, CA, USA), followed by assembly of the resulting constructs into the pLX-AS vector as described previously. The presence of the inserts in the PpVQ_V2 genome was

determined by RT-PCR using primers flanking the insertion site (Online Resource 1), followed by Sanger sequencing of purified PCR products.

Results

Confirmation of genome terminal sequences

Sequencing of five independent 5'-RACE clones identified an additional guanosine (G) residue at the 5' terminus relative to the published PpVQ reference genome (GenBank accession no. MT113180), whereas the analysis of 3'-RACE revealed two distinct terminal sequences. The first (PpVQ_V1), recovered from two independent clones, was 14 nt shorter than the reference sequence, whereas the second (PpVQ_V2), recovered from three clones, was 20 nt longer than the published genome. Interestingly, the last 8 nt of PpVQ_V2 were identical to those of babaco virus Q (BabVQ; GenBank accession no. MT113181), a closely related Group 2/Class 1 umbra-like virus infecting the mountain papaya (*Vasconcellea × heilbornii*), locally known as babaco [3] (Fig. 1).

Infectivity of PpVQ infectious clones carrying alternative 3' termini

To determine whether differences in the 3' termini affected virus infectivity, two infectious clones representing each terminal variant (PpVQ_V1 and PpVQ_V2) were constructed and evaluated. In *N. benthamiana*, both variants were detected in systemic, non-agroinfiltrated leaves of all plants by 3 weeks post-infiltration (wpi). In papaya, infection rates at 3 wpi were 60% for PpVQ_V1 and 80% for PpVQ_V2; however, both variants were detected in all inoculated plants by 5 wpi. Infected *N. benthamiana* plants developed symptoms consisting of vein clearing and leaf abnormalities, including cupping, twisting, and development of heart-shaped leaves (Fig. 2), similar to those reported for CY1 in N. *benthamiana* [9]. In contrast, infected papaya plants remained symptomless throughout the one-year observation period. RT-qPCR analysis of normalized ΔCt values detected no statistically significant differences in viral RNA accumulation between the two variants at any sampling time (Welch's t-test; $P > 0.05$). Nevertheless, PpVQ_V2 consistently showed higher mean RNA accumulation than PpVQ_V1, with average fold differences of approximately 3-fold at 10 wpi and 18-fold at 15 wpi, whereas no difference was observed at 3 wpi.

To determine whether the alternative 3' termini were maintained during infection, 3' RACE was performed on systemically infected plants at 10 and 15 wpi. Sequencing confirmed the presence of the corresponding terminal sequence in plants infected with either PpVQ_V1 or PpVQ_V2, indicating that both 3' terminal variants remained stable during infection and supporting the existence of naturally occurring alternative 3' termini in PpVQ. PpVQ_V2 was selected for all subsequent VIGS experiments.

Identification of a VIGS insertion site

Sequence analyses identified several motifs (9–12 nt in length) with potential complementarity to local or long-distance sequences, consistent with the RNAfold predictions (Fig. 3). Among these, a 9-nt motif (5'-AAAACTTAA-3'; nt 3,409–3,417) within the PpVQ 3' UTR showed comparatively low sequence conservation among PpVQ relatives (not shown) and no detectable reverse-complement repeats. In predictions of both the complete genome and the 3' UTR alone, the motif occurred at the boundary between two well-defined structural elements (Fig. 3). The flanking regions exhibited high average base-pairing (ABP) probabilities (> 0.9) and low average positional entropy (APE < 0.1), whereas the 9-nt motif was predicted to remain predominantly unpaired (ABP < 0.1) while maintaining low positional entropy (APE ~ 0.1), indicating a well-defined local structural state. Based on this structural context, the nucleotide immediately upstream of the motif (nt 3,408) was selected as the insertion site for subsequent VIGS experiments.

Transient retention of PDS inserts

Three PDS-specific inserts of different lengths were designed. Two inserts (PDS-62 and PDS-110) exhibited predicted structures and ABP, APE, and minimum free energy (MFE) values comparable to those of naturally occurring but computationally predicted hairpins (Fig. 4).

All inserts incorporated into PpVQ_V2 (PpVQ_PDS-97/62/110) were RT-PCR detected in systemic, non-inoculated leaves beginning at 3 wpi in both papaya (6/10 plants) and *N. benthamiana* (10/10 plants, PDS-97 only). At 3 wpi, no evidence of mixed viral populations carrying alternative insert sequences was detected. However, by 5 wpi, most samples yielded a single PCR product corresponding in size to the viral genomic fragment lacking the PDS insert, indicating that insert-containing genomes had been largely replaced by genomes lacking the insert. In the remaining samples, two PCR products corresponding in size to the fragments with and without the insert were detected, indicating the coexistence of insert-containing and insert-lacking viral genomes (Fig. 5). Sanger sequencing confirmed the identity of both amplicons.

Interestingly, for PpVQ_PDS-97 the deletion did not occur precisely at the insert boundaries: the first 6 nt of the PDS insert were retained, whereas the remainder of the insert and the first 5 nt of the downstream viral sequence were deleted (Fig. 5). This modified junction was consistently detected in *N. benthamiana* through 7 wpi and in about ~ 40% of papaya plants through 15 wpi, indicating that the deletion pattern was stably maintained during continued virus replication.

Although the characteristic photobleaching phenotype expected from effective PDS silencing was not observed, at 3 to 5 wpi PpVQ_PDS-97 infected *N. benthamiana* plants exhibited enhanced chlorosis together with the vein clearing, leaf cupping, and leaf distortion (Fig. 6), which were previously observed in plants infected with PpVQ_V1/V2. Papaya plants infected with PpVQ_PDS-97/62/110 remained symptomless throughout the experiment, with no evidence of photobleaching or other visible phenotypes indicative of PDS silencing.

Discussion

The present study provides new insights into the terminal sequence organization, infectivity, and genome plasticity of PpVQ, while also evaluating its potential as a virus-induced gene silencing (VIGS) vector.

The identification of two distinct 3' termini suggests that alternative terminal configurations may occur in PpVQ. Both variants were recovered from independent RACE clones, remained stable during systemic infection, and supported systemic infection in papaya and *N. benthamiana*. Terminal heterogeneity has also been documented in other umbra-like viruses. For instance, direct RNA sequencing of CY1 and CY2 revealed abundant viral RNAs with distinct 3' terminal configurations, including recurrent truncations [18], while analysis of grapevine umbra-like virus 4 (GULV4) showed that viral RNAs recovered from infected plants contained three terminal cytidines despite the infectious construct containing only two [19]. Notably, PpVQ_V2 shared an 8-nt terminal sequence with the related BabVQ, despite limited overall conservation of the 3' UTRs among these viruses. Although the significance of this shared sequence remains unclear, its conservation between related viruses raises the possibility of a functional role in genome replication or stability.

The contrasting phenotypes observed in *N. benthamiana* and papaya further suggest that PpVQ–host interactions may be strongly host dependent. PpVQ infection induced vein clearing and leaf distortion in *N. benthamiana*, whereas papaya plants remained symptomless for one year despite persistent systemic infection. A similar pattern has been reported for the closely related Group 2 umbra-like virus CY1, where infection of *N. benthamiana* produced pronounced leaf abnormalities, whereas CY1-infected citrus plants remained asymptomatic despite systemic infection [8]. Likewise, BabVQ has been detected in symptomless babaco plants, consistent with our observations of PpVQ in papaya [20]. This parallel raises the possibility that papaya and babaco represent relatively tolerant hosts for PpVQ and BabVQ, respectively, analogous to citrus for CY1, whereas infection of *N. benthamiana* elicits a more conspicuous host response. Although additional sampling and experimental host-range studies are needed to establish these host associations, the recurrence of these viruses in Caricaceae suggests that members of this family may represent an important ecological host group for PpVQ and related umbra-like viruses.

The structural analysis used to identify a potential VIGS insertion site illustrates the importance of considering both sequence conservation and RNA secondary structure when modifying viral genomes. The selected site was located at the boundary between two predicted structural elements, while the targeted 9-nt motif was predicted to remain predominantly unpaired and to have low positional entropy. Thus, the region represented a relatively well-defined local structural state rather than an unconstrained sequence. The intention was to introduce the PDS sequences at a position predicted to minimize disruption (e.g. maintain a low plasticity) of the surrounding viral RNA structure as suggested before [9, 21]. Although computational predictions cannot establish the structure adopted by the viral RNA in vivo, the combined sequence and structural criteria provided a rational basis for selecting the insertion site.

The subsequent behavior of the PDS inserts closely resembles that reported for the umbra-like virus CY1, in which PDS-derived hairpins were initially tolerated but underwent substantial deletions within a few weeks of infection in *N. benthamiana* [9]. In PpVQ, all three inserts were detectable in systemic tissues at 3 wpi, demonstrating that the virus can initially tolerate their incorporation and systemic movement. By 5 wpi, however, most samples contained predominantly insert-lacking genomes, while the remaining samples contained both insert-containing and insert-lacking genomes, indicating progressive selection for viral genomes carrying deletions within the inserted region. In the CY1 system, Simon and colleagues attributed similar insert instability to differences between the thermodynamic properties of foreign sequences and those of native viral RNA substructures, with inserts more closely matching the structural and thermodynamic properties of natural viral hairpins showing substantially greater stability [9]. Given the short-term retention of the PDS inserts in PpVQ, no characteristic photobleaching phenotype was observed in either *N. benthamiana* or papaya. Although some *N. benthamiana* plants infected with PpVQ_PDS-97 exhibited enhanced chlorosis at 3–5 wpi, papaya plants remained symptomless throughout the observation period. In contrast, Tuo et al. (2021) successfully induced PDS silencing in papaya using a 348-bp PDS fragment carried by papaya leaf distortion mosaic virus (PLDMV). Photobleaching became evident as early as 20 days post-inoculation and intensified by 35 days, while the PDS insert was largely maintained through 60 days post-inoculation [22]. Thus, the absence of a PDS-silencing phenotype in our study is unlikely to reflect an inherent limitation of PDS-based VIGS in papaya, but rather may be related to the rapid loss of the PDS inserts from the PpVQ genome before sufficient or sustained silencing could be established.

Although our findings do not support PpVQ as a stable VIGS vector under the conditions and genomic configuration tested here, they demonstrate that PpVQ can accommodate heterologous sequences sufficiently to permit their systemic movement for several weeks before strong selection for deletion occurs. This transient retention provides a starting point for further evaluation of PpVQ as a VIGS vector, including the testing of alternative insertion sites, shorter inserts, and genomic regions with greater tolerance for foreign sequences. Future studies using additional independent insertions, deep sequencing of viral populations, and comparative analysis of deletion junctions could determine whether the observed deletion pattern reflects a specific feature of PpVQ genome architecture or a more general mechanism of selection against heterologous sequences. As the type member of Group 2/Class 1 umbra-like viruses, PpVQ also provides an opportunity to investigate the relationship between viral RNA structure and genome stability. Experimental characterization of its RNA secondary structure, for example using SHAPE-based approaches, would be particularly valuable for identifying structural features that may constrain or favor the maintenance of foreign sequences [23]. More broadly, our findings highlight the importance of evaluating insert stability independently of viral infectivity and systemic movement when assessing candidate plant virus vectors, while providing new insights into the genomic flexibility and constraints of PpVQ and related umbra-like viruses.

Declarations

Acknowledgements

The authors gratefully acknowledge Dr. Fabio Pasin for his valuable insights and helpful discussions during the development of this study.

Funding

The authors declare that no funds, grants, or other support were received during the preparation of this manuscript.

Competing Interests

The authors have no relevant financial or non-financial interests to disclose.

Author contributions

The study was conceptualized and designed by Diego F. Quito-Avila and Robert A. Alvarez-Quinto. Material preparation, data collection and analysis were performed by Nelson Cubi-Insuaste, Milenka Vera, Sara Zurita, Raúl Cifuentes. The first draft of the manuscript was written by Diego F. Quito-Avila and all authors commented on previous versions of the manuscript. All authors read and approved the final manuscript.

Data availability

The datasets analysed during the current study are available in the GenBank repository under accession number MT113180. https://www.ncbi.nlm.nih.gov/nuccore/MT113180

References

1. Quito-Avila DF, Alvarez RA, Ibarra MA, Martin RR. Detection and partial genome sequence of a new umbra-like virus of papaya discovered in Ecuador. European Journal of Plant Pathology. 2015;143(1):199-204. doi: 10.1007/s10658-015-0675-y.
2. Cornejo-Franco JF, Alvarez-Quinto RA, Quito-Avila DF. Transmission of the umbra-like Papaya virus Q in Ecuador and its association with meleira-related viruses from Brazil. Crop Protection. 2018;110:99-102. doi: https://doi.org/10.1016/j.cropro.2018.04.006.
3. Cornejo-Franco JF, Flores F, Mollov D, Quito-Avila DF. An umbra-related virus found in babaco (Vasconcellea × heilbornii). Arch Virol. 2021;166(8):2321-4. Epub 2021/05/29. doi: 10.1007/s00705-021-05117-8. PubMed PMID: 34046760.
4. Simon AE, Quito-Avila DF, Bera S. Expanding the Plant Virome: Umbra-Like Viruses Use Host Proteins for Movement. Annu Rev Virol. 2024;11(1):283-308. Epub 2024/06/15. doi: 10.1146/annurev-virology-111821-122718. PubMed PMID: 38876114.
5. Huaman-Pilco AF, Tineo D, Guelac-Santillan M, Zamorano A, Bustamante DE. First report of babaco virus Q infecting babaco (Vasconcellea heilbornii) in Amazonas, Peru. New Disease Reports. 2025;52(1):e70046. doi: https://doi.org/10.1002/ndr2.70046.

6. Quito-Avila DF, Reyes-Proaño E, Cañada G, Cornejo-Franco JF, Alvarez-Quinto R, Moreira L, et al. Papaya Sticky Disease Caused by Virus "Couples": A Challenge for Disease Detection and Management. Plant Dis. 2023;107(6):1649-63. Epub 2022/12/28. doi: 10.1094/pdis-11-22-2565-fe. PubMed PMID: 36572970.
7. Kwon S-J, Bodaghi S, Dang T, Gadhave KR, Ho T, Osman F, et al. Complete Nucleotide Sequence, Genome Organization, and Comparative Genomic Analyses of Citrus Yellow-Vein Associated Virus (CYVaV). Front Microbiol. 2021;Volume 12 - 2021. doi: 10.3389/fmicb.2021.683130.
8. Ying X, Bera S, Liu J, Toscano-Morales R, Jang C, Yang S, et al. Umbravirus-like RNA viruses are capable of independent systemic plant infection in the absence of encoded movement proteins. PLoS Biol. 2024;22(4):e3002600. Epub 2024/04/25. doi: 10.1371/journal.pbio.3002600. PubMed PMID: 38662792; PubMed Central PMCID: PMCPMC11081511 is also a co-founder of Silvec Biologics, which has licensed the CY1 technology from the University of Maryland for development of a virus induced gene silencing vector, and has a financial interest in its success. SY is a Principal Research Scientist and JH is a Research Technician at Silvec Biologics and have a financial interest in its success.
9. Jang C, Needham JM, Johnson PZ, Gao F, Simon AE. Hairpin inserts in viral genomes are stable when they conform to the thermodynamic properties of viral RNA substructures. J Virol. 2025;99(4):e0191924. Epub 2025/03/21 20:03. doi: 10.1128/jvi.01919-24. PubMed PMID: 40116513; PubMed Central PMCID: PMCPMC11998532.
10. Wayne Hughes D, Galau G. Preparation of RNA from cotton leaves and pollen. Plant Molecular Biology Reporter. 1988;6(4):253-7. doi: 10.1007/BF02670385.
11. Halgren A, Tzanetakis IE, Martin RR. Identification, Characterization, and Detection of Black raspberry necrosis virus. Phytopathology. 2007;97(1):44-50. Epub 2008/10/24. doi: 10.1094/phyto-97-0044. PubMed PMID: 18942935.
12. Quito-Avila DF, Martin RR. Real-time RT-PCR for detection of Raspberry bushy dwarf virus, Raspberry leaf mottle virus and characterizing synergistic interactions in mixed infections. J Virol Methods. 2012;179(1):38-44. Epub 2011/10/05. doi: 10.1016/j.jviromet.2011.09.016. PubMed PMID: 21968094.
13. Livak KJ, Schmittgen TD. Analysis of relative gene expression data using real-time quantitative PCR and the 2(-Delta Delta C(T)) Method. Methods. 2001;25(4):402-8. Epub 2002/02/16. doi: 10.1006/meth.2001.1262. PubMed PMID: 11846609.
14. Pasin F. Assembly of plant virus agroinfectious clones using biological material or DNA synthesis. STAR Protocols. 2022;3(4):101716. doi: https://doi.org/10.1016/j.xpro.2022.101716.
15. Vera M, Cifuentes R, Keener R, Olszewski N, Alvarez-Quinto RA, Quito-Avila DF. Characterization of an unusual carlavirus-like RNA from papaya (Carica papaya) lacking essential genes. PLOS ONE. 2025;20(8):e0329708. doi: 10.1371/journal.pone.0329708.
16. Johnson PZ, Simon AE. RNAcanvas: interactive drawing and exploration of nucleic acid structures. Nucleic Acids Research. 2023;51(W1):W501-W8. doi: 10.1093/nar/gkad302.

17. Mikkelsen AA, Gao F, Carino E, Bera S, Simon Anne E. -1 Programmed ribosomal frameshifting in Class 2 umbravirus-like RNAs uses multiple long-distance interactions to shift between active and inactive structures and destabilize the frameshift stimulating element. Nucleic Acids Research. 2023;51(19):10700-18. doi: 10.1093/nar/gkad744.
18. Johnson Philip Z, Needham Jason M, Lim Natalie K, Simon Anne E. Direct nanopore RNA sequencing of umbra-like virus-infected plants reveals long non-coding RNAs, specific cleavage sites, D-RNAs, foldback RNAs, and temporal- and tissue-specific profiles. NAR Genomics and Bioinformatics. 2024;6(3). doi: 10.1093/nargab/lqae104.
19. Simon AE, Needham JM, Mikkelsen A, Atallah O. Structural and phylogenetic analyses of umbravirus and umbra-like virus genomes suggest evolution of capsid-like proteins from 30K movement proteins. Journal of Virology. 2026;100(4):e02209-25. doi: doi:10.1128/jvi.02209-25.
20. Cornejo-Franco JF, Medina-Salguero A, Flores F, Chica E, Grinstead S, Mollov D, et al. Exploring the virome of Vasconcellea x heilbornii: the first step towards a sustainable production program for babaco in Ecuador. European Journal of Plant Pathology. 2020;157(4):961-8. doi: 10.1007/s10658-020-02037-2.
21. Maeda Y, Mizuuchi R, Shigenobu S, Shibai A, Kotani H, Furusawa C, et al. Experimental evidence for the correlation between RNA structural fluctuations and the frequency of beneficial mutations. Rna. 2022;28(12):1659-67. Epub 2022/10/05. doi: 10.1261/rna.079291.122. PubMed PMID: 36195345; PubMed Central PMCID: PMCPMC9670806.
22. Tuo D, Yan P, Zhao G, Cui H, Zhu G, Liu Y, et al. An efficient papaya leaf distortion mosaic potyvirus vector for virus-induced gene silencing in papaya. Horticulture Research. 2021;8(1):144. doi: 10.1038/s41438-021-00579-y.
23. Low JT, Weeks KM. SHAPE-directed RNA secondary structure prediction. Methods. 2010;52(2):150-8. Epub 2010/06/18. doi: 10.1016/j.ymeth.2010.06.007. PubMed PMID: 20554050; PubMed Central PMCID: PMCPMC2941709.

Figures

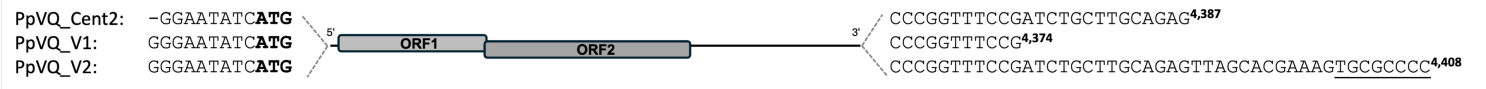


Figure 1

Terminal nucleotide sequences of papaya virus Q (PpVQ). The 5' and 3' terminal sequences of the reference isolate (Cent2) used in this study (GenBank MT113180) are shown together with those of two variants (PpVQ_V1 and PpVQ_V2) identified by RACE in this study. Bold nucleotides indicate the start codon, located at genome position 9 in Cent2 and position 10 in PpVQ_V1 and PpVQ_V2. Underlined nucleotides in PpVQ_V2 indicate the identical terminal sequence shared with babaco virus Q (BabVQ), a

related virus infecting mountain papaya (*Vasconcellea × heilbornii*) (GenBank MT113181). Superscript numbers indicate the complete genome length of each sequence

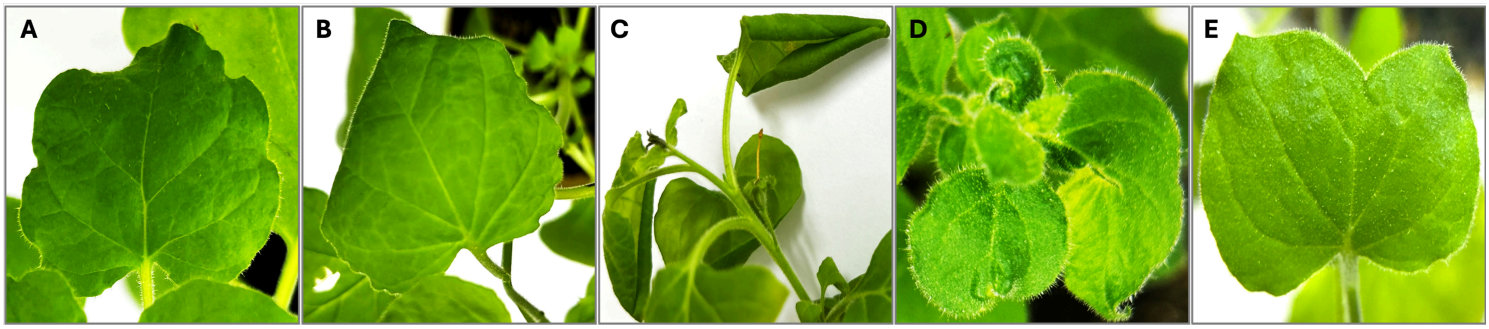


Figure 2

Papaya virus Q (PpVQ)-associated symptoms in *N. benthamiana*. Representative symptoms observed in *N. benthamiana* leaves at 3 weeks post agroinfiltration. No discernible differences in symptomatology were observed between PpVQ variants (PpVQ_V1 and PpVQ_V2). For comparison, a typical leaf from a non-agroinfiltrated plant is shown (A). PpVQ-associated symptoms included vein clearing (B), leaf cupping (C), leaf twisting (D), and heart-shaped leaves (E). All symptoms (B-E) were observed in systemic, non-agroinfiltrated leaves positive for PpVQ_V1 or PpVQ_V2

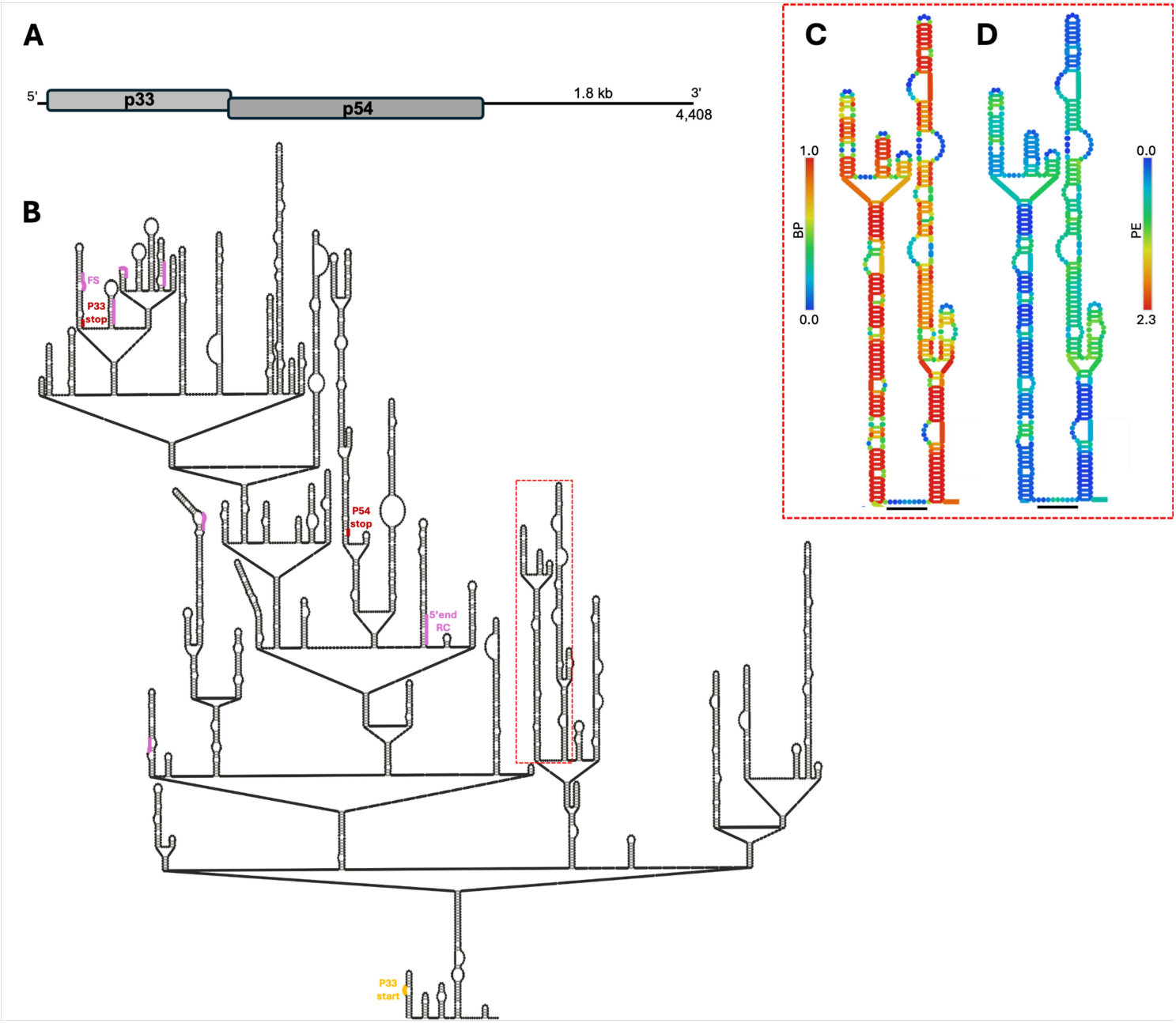


Figure 3

Genome organization of papaya virus Q (PpVQ_V2) and RNAfold-predicted RNA secondary structure. (A) Open reading frames (ORFs), showing the predicted molecular weight (kDa) of each protein. The long (~1.8-kb) 3' untranslated region (UTR) is indicated. (B) Schematic representation of the RNAfold-predicted secondary structure of the complete PpVQ genome. Genomic features, including start and stop codons and the putative heptameric slippery sequence associated with frameshifting (FS), are indicated. Additional predicted reverse-complement motifs are shown in pink. The region enclosed by the dotted rectangle is magnified in (C) and (D), showing the same region colored according to base-pairing (BP) probabilities (C), with red indicating high probabilities and blue low probabilities, and positional entropy (PE) (D), with blue indicating low PE and red high PE. The 9-nt non-interacting sequence (NIS) (5'-AAAACTTAA-3'), selected as the insertion site, is highlighted in (C) and (D)

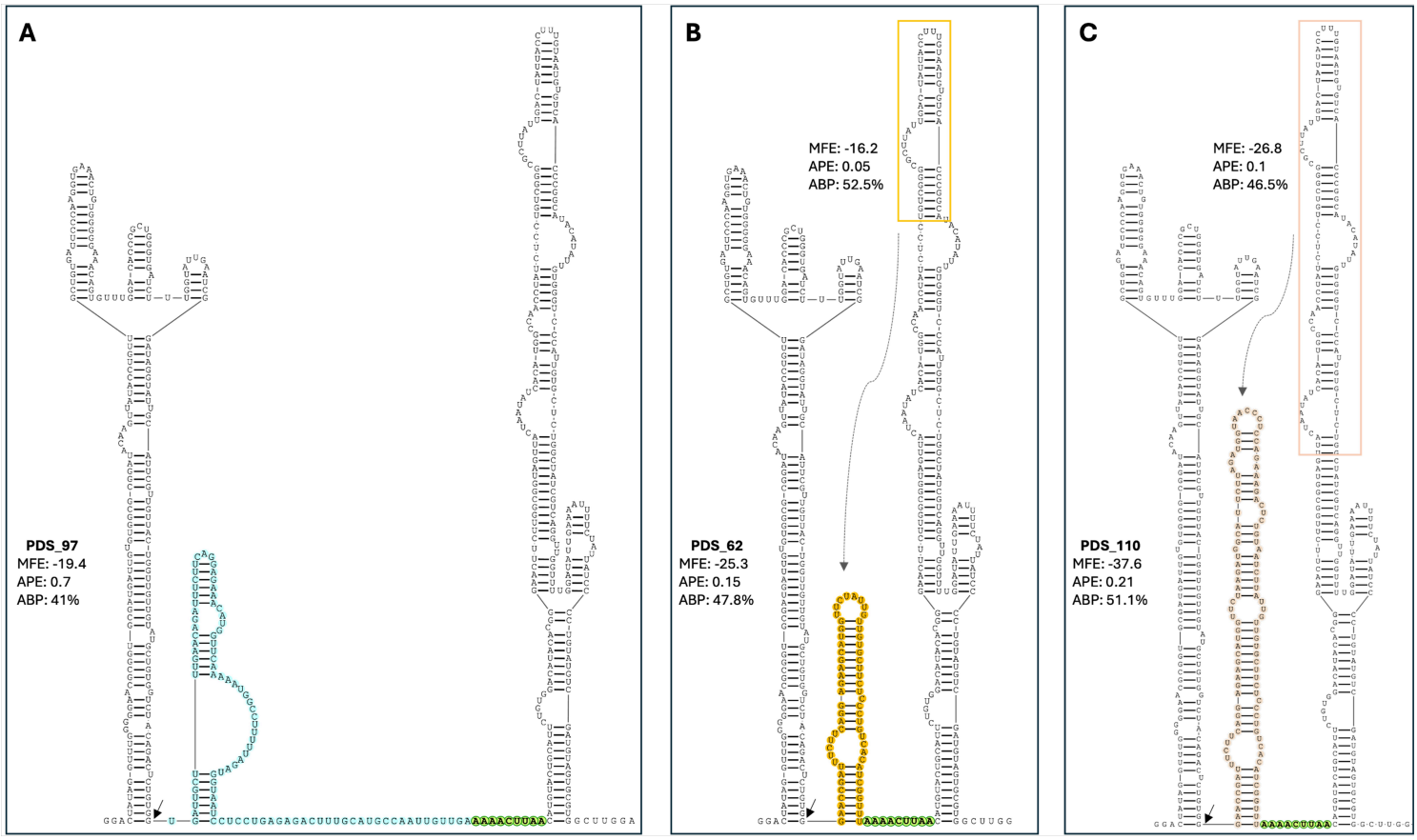


Figure 4

Predicted secondary structures of PDS inserts within the PpVQ genome. The predicted structures of three inserts of 97, 62, and 110 nt (PDS-97, PDS-62, and PDS-110) are shown in cyan (A), orange (B), and light brown (C), respectively. The inserts were introduced at genome position 3,408 (arrow). Green-circled nucleotides denote the non-interacting sequence (NIS; positions 3,409–3,417), located between two well-defined structural elements. RNAfold-derived minimum free energy (MFE), average positional entropy (APE), and average base-pairing probability (ABP), for each insert within the predicted whole-genome structure are provided. MFE, APE, and ABP values are also provided next to selected regions corresponding to natural PpVQ structures (B and C), which were used as structural models for the PDS-62 and PDS-110 hairpins (dotted curved arrows), respectively. In contrast, PDS-97 was designed without mimicking a natural PpVQ hairpin

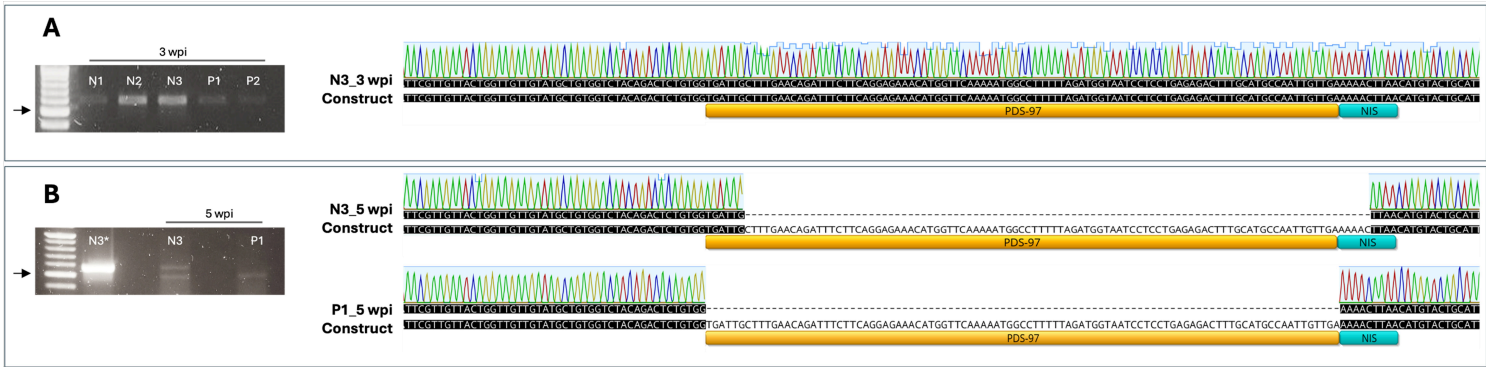


Figure 5

Transient retention of PDS-97 inserts in agroinoculated *N. benthamiana* and papaya. PCR amplification of a 591-nt fragment flanking the 97-nt PDS insert from selected samples of *N. benthamiana* (N1–N3) and papaya (P1–P2), followed by Sanger sequencing. (A) Amplified fragments at 3 weeks post agroinfiltration (wpi). The sequence alignment indicates the presence of the insert in a selected sample relative to the parental construct. (B) Amplified fragments from two samples, N3 and P1, at 5 wpi, along with the N3 sample at 3 wpi (N3*) as a reference for distinguishing the sizes of the bands. Note the double band in N3 at 5wpi, indicative of the presence of both insert-retaining and insert-deleted forms, whereas P1 shows a single ~490-nt band corresponding to a fragment in which the insert was deleted. The alignment shows two post-deletion forms: one (N3_5 wpi) in which deletion did not occur precisely at the insert boundaries, with the first 6 nt of the PDS insert retained, whereas the remainder of the insert and the first 5 nt of the downstream viral non-interacting sequence (NIS) were deleted; and a second (P1_5 wpi) in which insert deletion occurred precisely at the boundaries. The arrow indicates the position of the 500-bp band in the DNA ladder (FastGene® 100-bp DNA marker)



Figure 6

Phenotypic responses of *N. benthamiana* plants following agroinoculation with PDS-97 containing papaya virus Q (PpVQ_PDS-97). Enhanced vein clearing (A), leaf cupping (B), and chlorosis (C) observed in selected plants at 3 – 5 weeks post agroinfiltration. Note that (C) shows two chlorotic leaves from the same plant, illustrating the systemic nature of the response

Supplementary Files

This is a list of supplementary files associated with this preprint. Click to download.

- OnlineResource1.pdf